Semiautomatic Segmentation of the Cochlea Using Real-Time Volume Rendering and Regional Adaptive Snake Modeling

By Sun K. Yoo, Ge Wang, Jay T. Rubinstein, and Michael W. Vannier

The human cochlea in the inner ear is the organ of hearing. Segmentation is a prerequisite step for 3-dimensional modeling and analysis of the cochlea. It may have uses in the clinical practice of otolaryngology and neuroradiology, as well as for cochlear implant research. In this report, an interactive, semiautomatic, coarse-to-fine segmentation approach is developed on a personal computer with a real-time volume rendering board. In the coarse segmentation, parameters, including the intensity range and the volume of interest, are defined to roughly segment the cochlea through user interaction. In the fine segmentation, a regional adaptive snake model designed as a refining operator separates the cochlea from other anatomic structures. The combination of the image information and expert knowledge enables the deformation of the regional adaptive snake effectively to the cochlear boundary, whereas the real-time volume rendering provides users with direct 3-dimensional visual feedback to modify intermediate parameters and finalize the segmentation. The performance is tested using spiral computed tomography (CT) images of the temporal bone and compared with the seed point region growing with manual modification of the commercial Analyze software. Our method represents an optimal balance between the efficiency of automatic algorithm and the accuracy of manual work.

KEY WORDS: cochlea, spiral computed tomography, segmentation, real-time volume rendering, snake modeling.

THE HUMAN EAR transfers the sound wave from the environment to the hearing center in the brain in a limited space, consisting of the external, middle, and inner ear. Particularly, the cochlea in the inner ear is a tube of bone curled into a snail shape, which is about the size of a pea. The cochlea plays a critical role in transforming the vibratory movement of the sound energy into the electrical signal for sound perception. Therefore, anatomic knowledge of the cochlea is essential to the clinical practice of otolaryngology and neuroradiology, as well as research on cochlear implantation, the standard treatment for the profound deafness.[1-3] Many studies visualize and analyze the cochlear geometry with computer image processing for education, research, and treatment.[1,3-8] Recent advances of spiral computed tomography (CT) technology enable the production of high-resolution images of the cochlea in the 3-dimensional (3D) space.[8,9]

Segmentation of the cochlea is a prerequisite for a variety of image analysis and visualization tasks. It often is performed by commercial software using existing algorithms such as region growing, thresholding, boundary detection, and morphologic filtering.[3-8] However, incomplete segmentation occurs frequently because of several difficulties. First, partial volume artifacts caused by a small gap between voxels compromise spiral CT image resolution. It leads to ambiguous boundaries and mixed voxels. Second, adjacent structures connected to the cochlea have similar intensity distributions. As a result, the cochlea cannot be separated easily from other interconnected structures. Third, submillimeter sized cochlear features are in a complex 3D arrangement within the temporal bone. Hence, localization of the cochlea from a large number of sectional images represents a major challenge.

The manual modification method is the most common way of segmentation in cases of incomplete automatic segmentation.[4-7,10] It is a time-consuming and tedious task because extensive user interaction is involved to modify the incorrectly segmented border on each sectional image. It also requires experienced users to carefully define the cochlea because of the complexity of temporal bone structures. Nevertheless, resultant rendered surfaces still appear uneven.

Many segmentation approaches exist for elimination of the labor-intensive work of the manual method. One of them is the deformable active

From the Department of Medical Engineering, Yonsei University College of Medicine, Seoul, Korea and The University of Iowa School of Medicine, Iowa City, IA.

This work was supported in part by the Yonsei University Faculty Scholarship for Foreign Visiting Research and the National Institutes of Health (DC03590).

Address reprint requests to Sun K. Yoo, PhD, Department of Medical Engineering, The College of Medicine, Yonsei University, 120-752 Sudaemoon-Gu, Shinchon-Dong 134, Seoul, Korea.

0897-1889/01/1404-0004$35.00/0

contour model, which also is referred to as the *snake model.*[10-15] It has been applied successfully to a variety of image segmentation tasks, but it still requires user interaction to locate the initial contour and adjust internal parameters of the model. Another approach is the knowledge-based automatic segmentation tuned specifically to a particular human organ.[16] However, it is thought generally to be extremely difficult to formalize complex knowledge of the human anatomy. A promising alternative is the interactive segmentation, facilitating users to guide the segmentation process based on 3D visual feedback.[17,18] Instead of relying on poorly represented knowledge, it utilizes an expert's judgement. Although the feasibility and utility of the interactive segmentation approach have been shown in CT and magnetic resonance (MR) image segmentation, the obstacles for wide applications are the much-increased computational power for real-time 3D visualization and the need for appropriate operators to resolve mixed structures.

In this report, a semiautomatic approach is proposed to segment the human cochlea from spiral CT images. The fundamental structure of our method is similar to other interactive segmentation methods,[17,18] but our algorithm is focused specially on the cochlea and combines the knowledge-based processing and the user-guided modification. More distinctively, it incorporates the real-time volume rendering capability available on the personal computer as well as the regional adaptive snake model. The performance of our semiautomatic segmentation method is tested using clinical spiral CT images of the temporal bone and compared with that of the manual modification after seed point region growing using the commercial Analyze software.[19]

MATERIALS AND METHODS

CT Data Acquisition

A spiral CT scanner (Siemens Somatom PLUS-S, Siemens Medical Systems, Iselin, NJ) was used for data acquisition. This scanner provides up to 32 consecutive 1-s scans. The detector collimation is selectable from 1 mm to 10 mm. A research spiral CT software package on the scanner allows for raw data interpolation from opposite neighboring rays (half-scan interpolation/180LI) and overlapping transverse reconstruction down to 0.1 mm.[3,9] Scanning was performed with 165 mA for 17 seconds at 120 kV, 1 mm collimation, 1 mm table increment, 512 × 512 0.1 mm pixels with 4,096 gray levels (12 bits), and 0.1 mm reconstruction interval.

PC System Configuration

The PC-based semiautomatic segmentation system consists of Pentium II personal computer (Dell Precision 410, Round Rock, TX) with a 128 Mbytes internal RAM (Random Access Memory), a 32 Mbytes 3D graphic card (Permedia 3, 3Dlabs Inc, Sunnyvale, CA) with an AGP (accelerated graphics port) interface, and a real-time volume-rendering board (VolumePro, Mitsubishi Electronic, Concord, MA)[20] with a PCI interface. The VolumePro board renders 256^3 volumes (8- or 12-bit voxels) with trilinear interpolation at the rate of 30 frames per second based on shared warp transformation with Phong shading.[21] Hardware supported functions supplied by the VolumePro are used for real-time user interaction, including an opacity lookup table, a 3D cursor, and clopping utilities. It is programmed in Visual C++ 6.0 with VLI (Volume Library Interface, Mitsubishi Electronic) and Open GL.[20]

Interactive Segmentation

The cochlear shape in each slice changes, depending on the slice location, individual cochlear features, and patient orientation during scanning. Because a fully automatic segmentation method does not produce satisfactory results, our design goal is to maximize the efficacy of the computer processing and minimize the workload of manual processing. The basic knowledge to be used in cochlear segmentation is that the outer surface of the human cochlea is fairly smooth.[22] The snake segmentation algorithm is considered appropriate for this application because it can control the smoothness and adjust the convergence property. However, the snake modeling requires human interactions, namely, adjustment of processing parameters and specification of an initial contour. It also cannot be operated well in mixed regions, in which edges to distinguish the cochlea are weak, and the intensity distribution of mixed structures is similar to that of the cochlea. The semiautomatic segmentation with a coarse-to-fine strategy is used to overcome the difficulties. In coarse segmentation, information for fine segmentation is extracted in a roughly segmented volume of interest (VOI), whereas useless structures are excluded. In fine segmentation, the output of coarse segmentation is refined, and the mixed structures are dissolved by an elaborated snake algorithm. In the 2 stages of segmentation, 3D visualization is performed in real time to supply direct visual feedback for a user's guidance of the entire process to achieve a high segmentation quality.

Coarse Segmentation

The functions of the coarse segmentation are to define the intensity range and the volume of interest of the cochlea from temporal bone CT images. The hardware-based volume rendering, opacity adjustment, clopping, and 3D cursoring are combined to meet the real-time requirement in the human-computer interaction. As shown in Fig 1, the first step is to find the cochlea from complex temporal bone structures. The transparent effect is adjusted when the 3D volume is rotated until the cochlea can be seen clearly. The histogram for the whole image is displayed after a wide step function with small opacity values is assigned to the opacity look-up table. The second step is to define the VOI by adjusting the x, y, and z range in a clopping window. The clopping effect is reflected directly in the volume-rendered image, so a VOI can be defined easily. After the

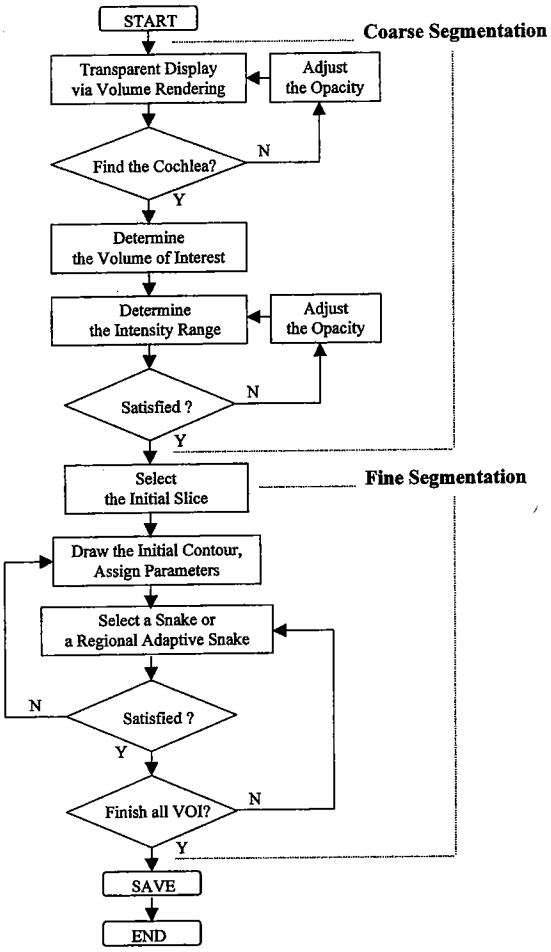

Fig 1. A flowchart of the procedure for interactive, semi-automatic segmentation.

clopping removes most of surrounding structures obscuring the cochlea, the final step is to determine the intensity range of the cochlea. The 2 edge points in the opacity step function, corresponding to the minimum and maximum gray-scale thresholds (th_1 and th_2), are adjusted until the volume-rendered image represents the proper cochlear structure.

Fine Segmentation

Either a snake or a regional adaptive snake model is used for fine segmentation to refine the output of the coarse segmentation and identify the cochlea from mixed surrounding structures.

Snake model. The energy functional used in the snake model is the sum of several terms, each corresponding to a type of force acting on a contour of interest.[10-15] In general, the snake is located initially near the contour of interest and is attracted to the target contour corresponding to the minimum of the functional. The contour for the snake model is represented by a vector, $V(s) = (x[s], y[s])$, parameterized by its arc length, s. The energy functional, E_{snake}, is defined as the sum of internal, external, and image energy.

$$E_{snake} = \int (E_{int} + E_{image} + E_{ext})ds \tag{1}$$

E_{int} represents the internal energy of the contour, typically containing terms of first and second derivatives.

$$E_{int} = \alpha\|V_s(s)\|^2 + \beta\|V_{ss}(s)\|^2 \tag{2}$$

The parameters, α and β, are used to balance the relative influence of the 2 terms. The first term minimizes the total length, whereas the second term requires the contour to be as smooth as possible. However, we can set $\alpha = 0$, if the snake points are well sampled to prevent shrinking and clustering problem of snake points.[11]

$$E_{image} = -\gamma\|\nabla G_\sigma * I(x,y)\| \tag{3}$$

E_{image} attracts the contour to strong edges with a suitably chosen weighting parameter, γ. Here G_σ and $I(x, y)$ denote a Gaussian smoothing filter of standard deviation σ, and the image intensity at (x, y), respectively. However, the gradient force sometimes is insufficient to attract the contour if it is not close enough to the boundary. Weak and false edges may mislead the contour. Also, spurious, isolated edge points may trap the contour.[13] Therefore, the contour should shrink or expand, depending on whether the snake is located outside or inside of the boundary, and should not be affected by weak and false edge.[12,13,15]

$$\frac{\delta E_{ext}}{\delta v} = \lambda F(x,y)n(s) \tag{4}$$

The external force term E_{ext} acts a force perpendicular to the contour on each point of a contour.[12,13] n(s) is the unit vector toward the outside of the contour. The parameter λ is the weighting factor to adjust the relative influence of the external force.

$$F(x,y) = \frac{1}{\eta}\sum_{(i,j)\in R} T(I(x-i, y-j))$$
$$T(I[x,y]) = 1 \quad \text{if } Th_1 \le I(x,y) \le Th_2, \tag{5}$$
$$T(I[x,y]) = -1 \quad \text{otherwise}$$

R denotes the neighborhood of a snake point at (x, y), η is the total number of pixels in R, and R is generally a 3 × 3 rectangular region.

The external force on a snake point is proportional to the ratio between the numbers of inside and outside pixels in R, with the direction controlled by the sign of the function F. If R is totally inside/outside the object ($F = 1/F = -1$), the maximum force moves the snake point in R toward outside/inside of the target boundary. The external force would be 0 if the numbers of inside and outside pixels in R are the same. The maximum external force makes the snake point move fast toward the border when the point is completely inside or outside the region, but the force is reduced gradually to 0 as the point approaches the border. The reduction of the external force prevents a snake point near the border from being moved away.

Regional adaptive snake model. The regional adaptive snake model copes with the incorrect convergence occurred in mixed regions, where the cochlea is connected to neighboring structures. It adopts the human knowledge used in the manual segmentation process. If the automatic segmentation fails in mixed regions, the expert would modify the undesirable cochlear boundary by smoothly outlining a border through the snake points of confidence. Most snake points move fast and stick to the cochlear boundary, whereas the other snake points oscillate or move slowly toward the border of neighboring structure in mixed regions. Weak and false edges produce gradient energy that disturbs the convergence process of the snake. Also, large discrepancies from the initial contour to the boundary of the cochlea reduce the speed of the convergence. Therefore, a regional adaptive snake model is designed not to take any effect until most snake points converge to the boundary of the cochlea. Then, such a regional model decreases the external and gradient forces and increases the internal force to reshape wandered points into a smooth curve in the uncertain regions. The regional adaptive snake model changes its parameters, β,γ, and λ, depending on the convergence property of each snake point and the intensity distribution in R.

$$\begin{aligned} \beta_R(s_i) &= \beta(1 + F[x,y]) \\ \gamma_R(s_i) &= \gamma(1 - F[x,y]) \\ \lambda_R(s_i) &= \lambda(1 - F[x,y]) \end{aligned} \tag{6}$$

if the number of converged snake points $\geq Th_c$ *and* s_i *is a nonconverged snake point*

Snake operation. The fine segmentation of sectional images is performed slice by slice.[13] As shown in Fig 1, a proper middle slice is selected for the initial contouring with preassigned parameters for the snake modeling. Before iteration, a user specifies either a snake or a regional adaptive snake, depending on whether mixed regions exist. Then, the converged snake contour propagates to adjacent slices as an initial contour, because there are no significant changes in the shape of the cochlea between adjacent slices in most cases. However, the contour carrying over is not satisfactory in some cases, because a given slice interval causes the split and merge of the cochlear shape from one slice to the next. The real-time volume-rendered image with a highlighted overlap of segmented sectional images facilitates the initialization of the snake in a new slice.

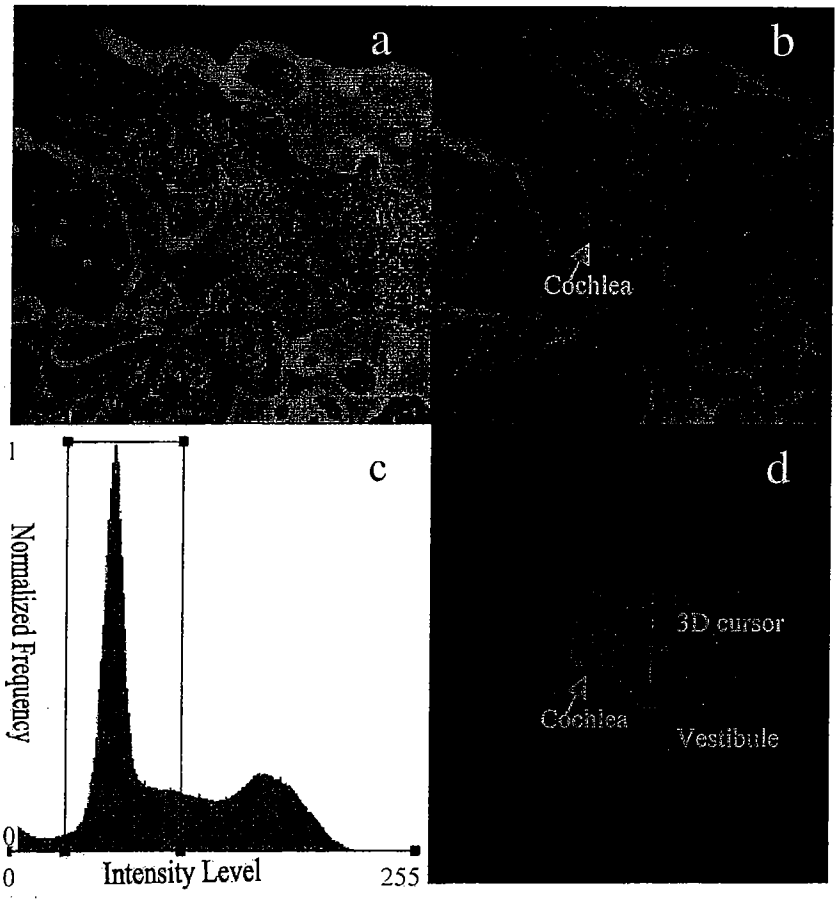

Fig 2. Coarse segmentation. (a) Opaque rendering, (b) transparent volume rendering with low opacity, (c) histogram for the entire image volume and a determined intensity range for the cochlea, (d) volume of interest.

RESULTS

A prototype system is implemented to test the performance of our semiautomatic method for cochlea segmentation. The subimages with the spatial resolution of 256 × 256 are selected from the original 512 × 512 pixel matrix size, and the intensity resolution of 12 bits is scaled down to 8 bits in the prototype system. Figure 2 shows a typical example of the coarse segmentation process. As shown in Fig 2a, it is extremely difficult to find the cochlea from the complicated temporal bone structures when opaque rendering (corresponding to surface rendering) is applied to the whole 3D data set. Comparing Fig 2a to Fig 2b, the advantage of volume rendering over surface rendering is that a simulated projection of semiopaque voxels yields an overlapped, transparent 3D display of multiple structures, enabling the cochlea to be found in complex temporal bone structures. After a clopping is applied to obtain the VOI (Fig 2d), the proper intensity range for the cochlea can be determined interactively which is 32 to 105 in this case. The volume rendered image (Fig 2c) provides a direct visual feedback in real time when the intensity range is changed. It can be observed in Fig 2d that coarse segmentation is insufficient to separate the cochlea in mixed regions, such as the vestibule and modiolus.

Figure 3a and d show 2 different initial contours roughly drawn: one is outside and the other is inside of the cochlea. As shown in Fig 3c and f, the conventional snake,[11,14] which uses a combination of the internal energy and the gradient energy, converges to either a neighboring border or high gradient points. It depends highly on the initial snake location.[10] However, the inclusion of the external force makes our model insensitive to the initial snake location, as shown in Fig 3B and E. Because the converged snake is used as the initial contour for the adjacent slice, the shrinkage/expansion of the snake is required to compromise the shape changes between slices.

In Fig 4, the performance of the regional adaptive snake model with $THc = 83\%$ is compared with that of the conventional snake model in mixed regions. In the conventional snake model, some snake points converge to neighboring boundaries of the vestibule and the modiolus, and 2 contours corresponding to the upper and lower turn bound-

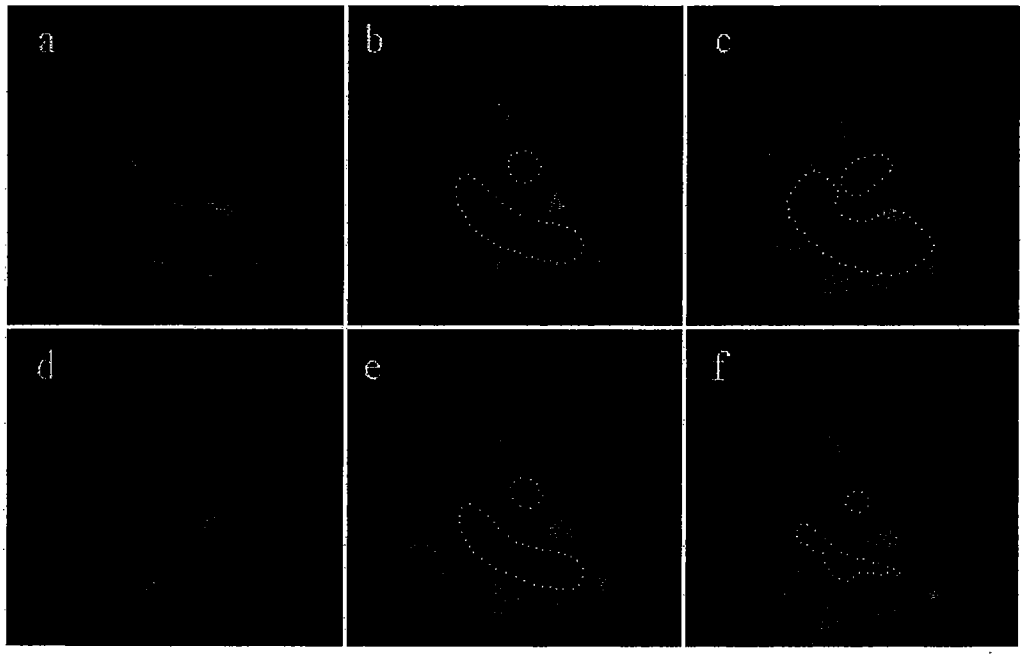

Fig 3. Snake convergence depending on the initial contour and energy forces. Black line and white dots represent the initial contour and converged snake points, respectively. (a, d) Initial contours, (b, e) converged snake with internal, gradient, and external energy terms, (c, f) converged snake with internal and gradient terms.

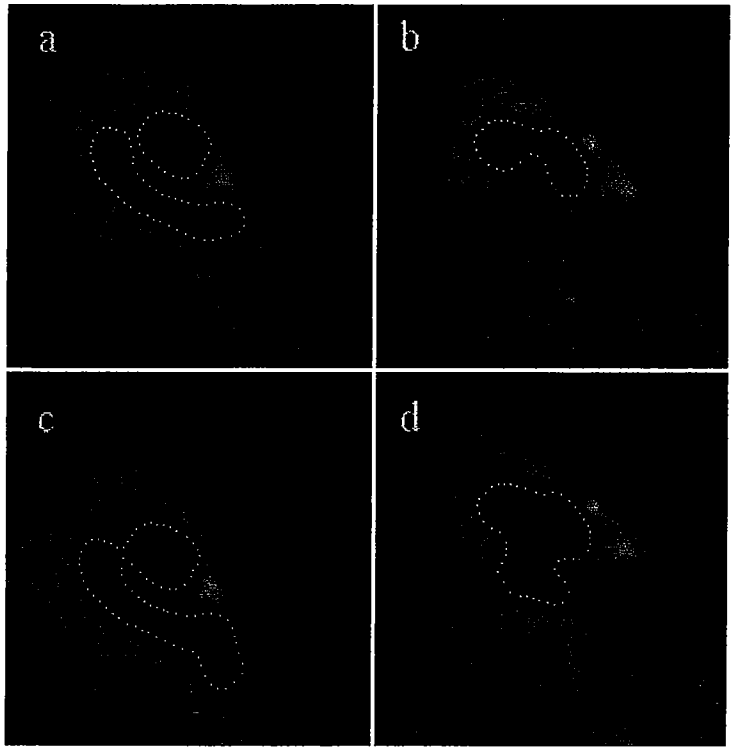

Fig 4. Converged contours of the snake and the regional adaptive snake in mixed regions with partial volume artifacts and similar intensity distributions. In the regional adaptive snake model, the cochlear boundaries can be shaped correctly, and the upper and lower turn boundaries are separated. (a, b) Regional adaptive snakes (c, d) conventional snakes.

aries of the cochlea are merged together, as shown in Fig 4c and d. In the regional adaptive snake model, the cochlear boundaries can be shaped correctly even in the mixed regions, and the upper and lower turn boundaries are separated, as shown in Fig 4a and b. Through iterations with the regional adaptive snake model after the percentage number of converged points exceeds the *THc*, the wandered snake points in mixed regions settle down to the smoothly reshaped cochlear boundary, which is consistent to what an expert outlines manually.

The performance of our semiautomatic segmentation is compared with that of the commercial software *Analyze* using seed-point region-growing with manual modification tools,[19] because specific segmentation algorithms for the cochlear are unavailable. The Analyze was installed on the Indigo II workstation (Silicon Graphics) with 128 Mbytes RAM. Three testing sets of spiral CT images from different patients were acquired by the spiral CT with the same protocol described the Data Aquisition section. During data acquisition, the modiolar axis was aligned to the table motion direction.[1,22] As summarized in Table 1, the total time of our segmentation method takes from 15 to 25 minutes, whereas that of Analyze takes 252 to 344 minutes. The automatic segmentations with both snake modeling and region-growing are completed within 1 second for all the sectional images; hence, the human-computer interaction takes most of the total segmentation time. The preparation time using Analyze is much longer than the coarse segmentation time using our semiautomatic system, because the Analyze does not provide a real-time visualization capability for determining key parameters, such as initial seed positions, an intensity range, and an initial region boundary. The major part of the user interaction is the number of failed slices. The mixed regions are responsible primarily for the failure of the automatic segmentation using Analyze. The failure with the regional adaptive

Table 1. The Performance Comparison Between Our Semiautomatic Segmentation and the Seed-Point Region-Growing With Manual Modification Using Analyze

	Case 1	Case 2	Case 3
Total number of slices	131	161	170
Number of slices of the cochlea	54	73	65
Analyze			
Preparation time (min)	70	85	90
Number of slices of successful automation	20	26	35
User interaction and computation time for successful slices (min)	7	9	12
Number of slices of failed segmentation	34	47	30
User interaction and computation time for failed slices (min)	180	250	150
Total time (min)	257	344	252
Coarse-fine semiautomatic segmentation			
Coarse segmentation time (min)	5	8	10
Number of slices of successful segmentation	49	65	59
User interaction and computation time for successful slices (min)	5	7	6
Number of slices of failed segmentation	5	8	6
User interaction and computation time for failed slices (min)	5	10	6
Total time (min)	15	25	22

snake modeling occasionally happens if the split-off or merging of the cochlear shape occurs between adjacent slices. The changed shape in mixed regions sometimes require readjustment of the *THc* parameter of the regional adaptive snake modeling. Overall, our system only requires a small amount of user interactions to readjust the internal parameters or the initial contour of the snake, whereas the manual modification process using Analyze takes a large amount of time for refinement of incorrect segmentation results.

The function of our semiautomatic segmentation is highly dependent on the region-adaptive snake model. Snake parameters, β,γ, and λ, fixed to predetermined values (1.5, 0.5 and 1.0, respectively), are robust to form the correct cochlear boundary in all the testing cases. A weak point is that the converged boundary in the mixed region slightly changes depending on the initial contour location and the *THc* parameter setting. The propagation of a converged snake contour from one slice to the next compromises the initial contour and *THc* dependency to some extent, but direct visual feedback as shown in Fig 5 provides an auxiliary means for the user interaction. The segmented section is overlapped on a volume-rendered image. The highlighted display of a segmented section helps users instantly judge the correctness of the segmentation. The 3D cursor also supplements the visual knowledge in the case of ambiguous boundaries.

The number of user interactions depends on the degree of shape variation between slices, but one or two trials are sufficient in all the testing cases, which takes up to 2 minutes. The snake instability results from the self-intersection of the snake contour. The frame buffer method[15] to check the self-intersection is performed every 3 iterations, then the snake points are redistributed to equal distance, 3 pixels wide.

The 3D visualization with the same rendering parameters is used to compare the segmentation

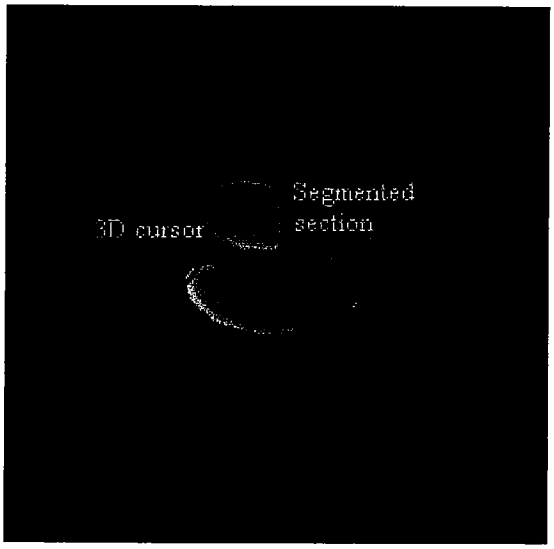

Fig 5. Fine segmentation. Segmented section and the 3D cursor are overlapped on a volume-rendered image.

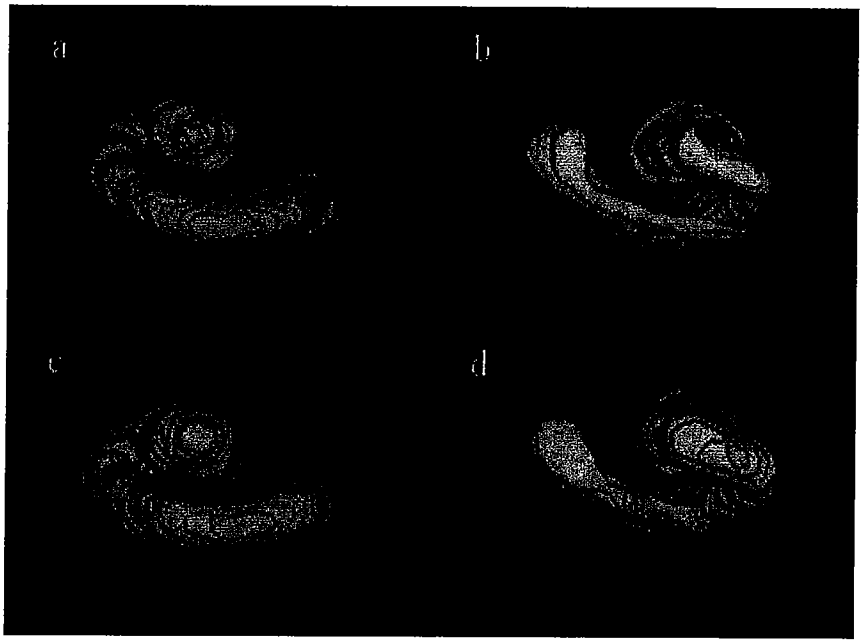

Fig 6. 3D volume-rendered views of the cochlea at 2 different orientations with the same rendering condition. (a, b) Segmentation performed by manual adjustment after seed-point region-growing using the Analyze software. (c, d) Segmentation performed using our method.

quality with our method (Fig 6c and d) and the Analyze method (Fig 6a and b). With Analyze, an expert carefully modifies failed results of the seed-point region-growing. Our method depicts the cochlear shape somewhat more smoothly than Analyze does, but with much less user interaction time. This is because the internal energy term in the snake model refines coarse segmentation effectively, whereas even an expert cannot smoothly modify every incorrectly segmented slice without direct 3D visual feedback.

DISCUSSION AND CONCLUSION

Semiautomatic segmentation systems using direct visual feedback have been applied to various medical images to reduce the time-consuming manual user interaction.[17,18] Commonly, they combine existing segmentation algorithms with 3D visualization to guide the segmentation procedures and have been advantageous over other automated segmentation algorithms in a number of applications. However, the 2 common problems with these systems are visualization in real time and separation of objects of interest from multiple overlapped/connected objects. Currently, the separation operators such as combined sequential processing with morphologic filters,[17] cut plane operator,[18] and sheet operator[23] are not appropriate for isolating the cochlea in mixed regions. The gradient in this region is too weak, and the intensity distributions of temporal bone structures are too similar. Also, mixed regions distribute widely and are not straight/flat. Our regional adaptive snake model is an elaborated, fine isolation operator adapted to the cochlea, which overcomes the above difficulties. The overall coarse-to-fine segmentation process represents an optimal combination of the efficiency of the automatic algorithm and the accuracy of the manual work.

An interactive, semiautomatic approach using a coarse-to-fine strategy has been developed on a general personal computer with real-time hardware rendering board for segmentation of the human cochlea from spiral CT images. In the coarse segmentation, the VOI and segmentation parameters are defined through real-time visualization. In the fine segmentation, a regional adaptive snake model is applied as a refining operator to separate the cochlea from mixed or ambiguous structures. The combination of image information and the expert's knowledge permits deformation of the snake contour satisfactorily to the cochlear boundary. The

PC-based implementation means a wide applicability of our semiautomatic segmentation system in hearing research, specifically in visualization and analysis of spiral CT images for cochlear implantation.

ACKNOWLEDGMENT

The authors thank Dr Margaret W. Skinner (Washington University) for providing the spiral CT images used in this study, and Dr R.A. Robb for the Analyze software (the Mayo Biomedical Imaging Resource, Rochester, MN).

REFERENCES

1. Kawano A, Seldon HL, Clark GM: Computer-aided three-dimensional reconstruction in human cochlear maps: Measurement of the lengths of organ of Corti, outer wall, inner wall, and Rosenthal's canal. Ann Otol Rhinol Laryngol 105:701-709, 1996

2. Loizou PC: Introduction to cochlear implants. IEEE Engineering in Medicine and Biology, Jan./Feb: 32-42, 1999

3. Wang G, Vannier MW, Skinner MW, et al: Unwrapping cochlear implants by spiral CT. IEEE Trans Biomed Eng 43:891-900, 1996

4. Seldon HL: Three-dimensional reconstruction of temporal bone from computed tomographic scans on a personal computer. Arch Otolaryngol Head Neck Surg 117:1158-1161, 1991

5. Takahashi H, Sando I: Computer-aided 3-D temporal bone anatomy for cochlear implant surgery. Laryngoscope 100:417-421, 1990

6. Frankenthaler R, Moharir V, Kikinis R, et al: Virtual Otoscopy. Computers in Otolaryngology 31:383-392, 1998

7. Yoo SK, Wang G, Rubinstein JT, et al: Three-dimensional modelling and visualization of the cochlea on the internet. IEEE Tran Info Tech in Biomed June, 2000

8. Himi T, Kataura A, Sakata M, et al: Three-dimensional imaging of the temporal bone using a helical CT scan and its application in patients with cochlear implantation. ORL; Journal of Oto-Rhino-Laryngology & its related specialties 58:298-300, 1996

9. Wang G, Vannier MW, Skinner MW, et al: Spiral CT image deblurring for cochlear implantation. IEEE Trans Med Imag 17:251-262, 1998

10. Yuan C, Lin E, Millard J, et al: Closed contour edge detection of blood vessel lumen and outer wall boundaries in black-blood MR images. Mag Res Imaging 17:257-266, 1999

11. Williams DJ, Shah M: A fast algorithm for active contours and curvature estimation. CVGIP: Image Understanding 55:14-26, 1992

12. Xu G, Segawa E, Tsuji S: Robust active contours with insensitive parameters. Pattern Recognition 27:879-884, 1994

13. Cohen LD: On active contour models and balloons. CVGIP:Image Understanding 53:211-218, 1991

14. Kass M, Witkin A, Terzopoulos D: Snakes: Active contour models. Int J Comput Vision 1:321-331, 1987

15. Ivins J, Porrill J: Statistical snakes: Active region models. Image and Vision Computing 13:431-438, 1995

16. Sonka M, Park W, Hoffman EA: Rule-based detection of intrathoracic airway trees. IEEE Trans Med Imag 15:314-326, 1996

17. Höhne KH, Hanson WA: Interactive 3D segmentation of MRI and CT volumes using morphological operations. J Comput Assist Tomogr 16:285-294, 1992

18. Salviroonporn P, Robatino A, Zahajszky J, et al: Real-time interactive three-dimensional segmentation. Acad Radiol 5:49-56, 1998

19. Robb RA et al: ANALYZE™ Reference Manual, Version 6.2, Biomedical Imaging Resource, Mayo Foundation, 1993

20. Real Time Visualization, VolumePro User's Guide, http://www.rtviz.com/, Mitsubishi, 2000

21. Lacroute P, Levoy M: Fast volume rendering using a shear-warp factorization of the viewing transformation. Proc SIGGRAPH'94, 1994

22. Ketten DR, Skinner MW, Wang G, et al: In vivo measures of cochlear length and insertion depth of nucleus cochlear implant electrode array. Ann Otol Rhinol Laryngol 107:1-16, 1998

23. Cleynenbreugel JV, Kratka D, Berben L, et al: A semi-automatic three-dimensional segmentation method for disarticulation of bone structures on spiral computed tomography images. J Digit Imaging 8:156-161, 1995